

Excess heat in a Pd(Pt)-D₂O+LiOD reflux open-electrolytic cell

Hui Zhao^{1,2}, Wu-Shou Zhang^{1,*}, Wu-Yun Xiao^{2,*}, Yang Sun¹

¹ *Institute of Chemistry, Chinese Academy of Sciences, P.O. Box 2709, Beijing 100190, China*

² *State Key Laboratory of NBC protection for Civilian, Beijing 102205, China*

Abstract

A heavy water reflux open-electrolytic cell was developed, which features a branch tube on the upper part of the cell for the gas outlet and condensed D₂O reflow, which differs from the isoperibolic cell used by Fleischmann-Pons and Miles. The evaporation rate (4.32I in µg/s) and power (9.79I in mW) of D₂O in open electrolysis at 25°C are small constants, which are almost independent from the atmosphere pressure, and the power balance is therefore simplified. Mass losses in D₂O electrolysis were measured, and the results verified that the actual amounts of evaporation were consistent with the theoretical values within 4% under careful design and operation. Excess power in the Pd(Pt)-D₂O+LiOD (H₂O+LiOH) cell were measured by a Seebeck envelope calorimeter with a higher sensitivity than our previous calorimeter. Four phenomena were observed: (1) Excess power was more readily observed in Pt-D₂O(H₂O) than in Pd-D₂O system. The maximum average excess power was 59 ± 7 mW with average input power of 2.5 W for Pt-D₂O system and 90 ± 3 mW with average input power of 1.5 W for Pt-H₂O system. The reasons are still unclear so far, and this phenomenon has puzzled us for quite a while because the Pt-D₂O(H₂O) cell was always considered the reference system in past experiments. (2) The maximum average excess power was 19 ± 9 mW with average input power of 4.1 W and 46 ± 3 mW with input power of 2.9 W for the Pd-Cu and Pd-B rods, respectively, provided by Melvin H. Miles. (3) The open electrolysis is in unsteady state, and this state can be divided into 2 categories – long-term shift (LTS) and short-term fluctuation (STF), which responds to the input power changing over time. For long-term shift, the instantaneous excess power must be compensated by the change rate of input power. For short-term fluctuation, the data logging rate cannot follow or reflect the changing of input power, and the input power is always overestimated; the resulted output power may be less than the input power for all cells. (4) The concentration of LiOD in the electrolyte decreased with time during electrolysis and it was found that LiOD had turned into a precipitate of Lithium silicate (Li₂SiO₃), which was verified by X-Ray Diffraction. All these factors make the calorimetry complicated, and the exact reproduction of excess heat in open-cells must be done carefully.

Keywords: Excess heat, Heavy water, Light water, Lithium deuterioxide, Lithium silicate, Mass loss, Palladium, Platinum, Reflux open-electrolytic cell, Thermoneutral potential.

1. Introduction





It is well known that excess heat occurred in Pd-D₂O system was found firstly in open-electrolytic cells by using isoperibolic calorimetry (IPC) by Fleischmann and Pons^[1,2] and repeated afterwards in closed-electrolytic cells with mass-flow calorimeter (MFC, e.g., McKubre et al.^[3]) and Seebeck envelope calorimeter (SEC, e.g., Storms^[4]). Since

*Corresponding author. E-mail: wzhang@iccas.ac.cn or zhangwushou@hotmail.com.

*Corresponding author. E-mail: xiaowuyun@sklnbpc.cn.

then, Melvin H. Miles has been studying excess heat in open Pd-D₂O electrolytic cells with IPC in detail for more than 30 years^[5–8]. During the satellite meeting of ICCF20 in 2016, Xing Zhong Li suggested Wu-Shou Zhang, one of the authors of this work to measure excess heat with the samples of Miles using the SEC. In May 2017, Miles mailed 4 samples to Zhang as listed in Table 1.

Table 1. Samples from M. H. Miles.

Pd #	Photo	Size, area, mass etc.	Notes of Miles
1	C#490, Mel Rod modified 	$\phi 6.35 \times 19.46$ mm ² , 4.5155 cm ² , 7.4046 g, rough sides, bright smooth ends	JM, production of excess heat and ⁴ He in China Lake. $P_{ex,max} = 0.52$ W. ^[5]
2	Pd-0.25 B 	$\phi 4.71 \times 20.1$ mm ² , 3.3227 cm ² , 4.1156 g, bright	New sample, Made at NRL by Dr. Imam. This batch gave excess heat in NHE. $P_{ex,max}$ = 0.35 W. ^[7]
3	Pd-Cu 	$\phi 4 \times 25$ mm ² , 3.393 cm ² , 2.7683 g, black and rough	Probably tested at NHE/Japan prior to 1997 (but was not Miles' experiment)
4	Pd wire 	$\phi 1 \times 30$ mm ² , 0.9582 cm ² , 0.2752 g, bright	JM, 1989, Batch W12954. Samples from this batch have given excess heat in many previous experiments. $P_{ex,max} = 0.073$ W. ^[6]

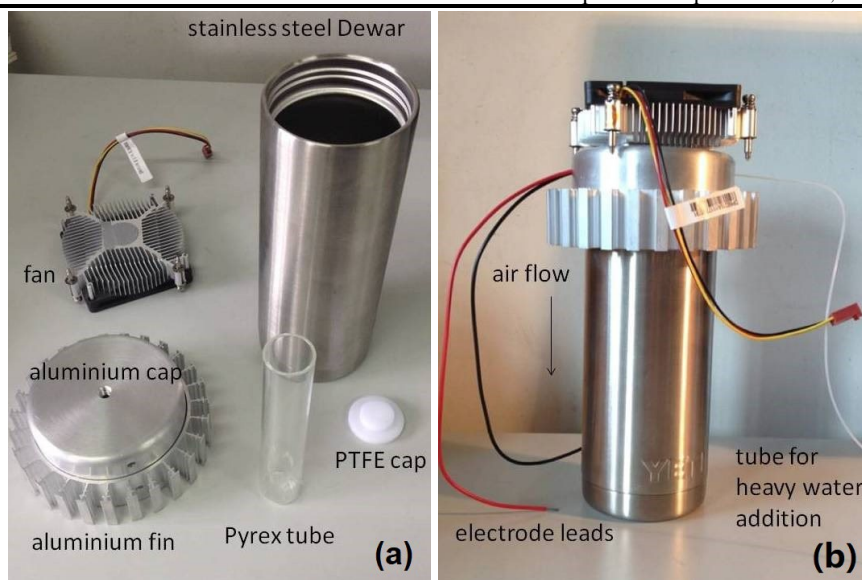


Figure 1. Different parts (a) and their assembly (b) of Pd(Pt)-D₂O+LiOD open-electrolytic cell from 2018 to 2019.

Because the sensitivity of our SEC was ~ 20 mW at that time^[9–13], which was worse than 0.1 mW of IPC used by Miles^[6], the SEC had to be improved first, as will be described in Section 3.1. From 2018 to 2019, the first generation open-electrolytic cell was tested as shown in Fig. 1. The cell was a Pyrex tube (49 ml capacity, $\phi_{in} 22$ mm \times 130 mm) with a PTFE lid. Both leads of cathode and anode were fixed onto the lid. The cathode was Pd#3 listed in Table 1 or Pt film with the same area, the anode and electrode leads were Pt wires. The cell with polyurethane foam wrapping around as heat insulation material was placed in the center of a stainless-steel Dewar, and an aluminum alloy lid with fins covered the Dewar. A fan was fixed on the Dewar top in a way to ensure that the air was blown downward and the temperature distribution was even in the SEC. The Dewar with fan was put in the center of the calorimeter. The

purpose of this design was to reproduce the electrolytic process in IPC of Miles and to measure the output power using the SEC.

We tested Pt and Pd#3 cathodes with D₂O+LiOD electrolyte using our SEC as listed in Table 2. In our test, excess power was obtained using the model developed by Fleischmann-Pons and Miles (F-P-M, the same below) [1,2,5-8], with the output power measured by their IPC being replaced with that by our SEC. However, we found that the Pt-D₂O system gave zero excess power at relatively low temperatures (< 63°C) and that both Pt-D₂O and Pd-D₂O systems gave prominent positive excess power at higher temperatures with a reproducibility in 4 out of 8 tests. But these results were too good to believe. After checking the design, we found the excess power mainly comes from the term of evaporation power of heavy water, P_{vapor} . In F-P-M situation, the vapor of heavy water escapes to air, which is the external environment of the IPC [1,2,5-8]. In our case, the vapor that escapes from the Dewar either condenses in the sample chamber of the SEC, or leaks out of it. This means the term P_{vapor} becomes an uncertainty value here. Therefore, the calorimetric results had a serious problem and we had to design a new cell to avoid it.

Table 2. Summary of excess heat in the Pd(Pt)-D₂O+LiOD open-electrolytic cell from 2018 to 2019.

Exp. #	Integrated values				Steady values					
	$I \times t$ A × h	Q_{in} kJ	Q_{ex} kJ	\bar{P}_{ex} mW	I mA	P_{in} W	P_{ex} mW	T_{bottom} °C	T_{up} °C	P_{vapor} mW
180911Pt	0.17×48	148.89(33)	−0.49(71)	−2(3)	171	0.381(1)	6(2)	48	NA	NA
	0.34×24				340	0.942(2)	−19(3)	73	NA	NA
181005Pt	0.17×60	114.68(30)	0.35(60)	2(3)	171	0.521(1)	12(3)	51	41	4
					171	0.539(3)	−1(3)	53	42	5
181017Pt	0.17×60	125.69(35)	0.64(63)	3(3)	171	0.578(2)	2(2)	48	39	4
					171	0.573(1)	7(2)	50	39	4
190414Pt	0.17×60	134.83(14)	−0.27(80)	−1(4)	170	0.614(2)	−7(3)	52	40	4
					170	0.638(2)	−4(3)	55	40	4
190502Pt	0.17×60	139.021(14)	−0.23(80)	−1(4)	171	0.638(1)	0(3)	51	41	4
					171	0.631(1)	5(3)	51	41	4
190507Pt	0.34×54	322.23(15)	−0.74(76)	−4(4)	341	1.566(2)	3(3)	76	63	31
190513Pt	0.51×19	239.50(7)	6.32(32)	92(5)	511	3.075(16)	178(20)	93	87	252
190816Pt	0.51×36	191.98(10)	−0.73(56)	−6(4)	511	1.423(4)	5(4)	72	52	25
					511	1.500(3)	5(3)	74	53	26
190904Pd3	0.15×24	188.77(10)	−6.71(52)	−78(6)	148	2.029(115)	−65(117)	82	67	17
					148	2.216(111)	−97(111)	87	69	20
190909Pd3	0.34×22	120.30(5)	−0.27(53)	−3(7)	340	1.207(38)	9(10)	69	50	15
190920Pd3	0.31×60	483.64(17)	−4.58(268)	−21(12)	228	1.522(97)	−24(119)	78	52	11
					228	2.006(59)	36(86)	85	63	21
191005Pd3	0.51×24	191.98(8)	1.64(134)	19(16)	511	2.212(13)	32(27)	78	65	52
191007Pd3	0.55×48	543.64(15)	14.79(220)	86(13)	550	3.060(15)	132(50)	87	76	118
					550	3.381(44)	88(44)	87	77	125
191010Pd3	0.47×48	619.40(17)	20.63(225)	119(13)	541	4.081(15)	182(33)	90	83	190
					360	3.317(24)	46(19)	84	71	55

* Meanings of symbols: I , electrolysis current; t , electrolysis time; Q_{in} , input energy; Q_{ex} , excess heat; P_{ex} , excess power; T_{bottom} , cell-bottom temperature; T_{up} , cell-up temperature; P_{vapor} , evaporation power of heavy water at T_{up} [1,2,5-8].

2. Experimental set-up and calorimetry of reflux open-electrolysis

2.1. Experimental set-up

We designed a reflux open-electrolytic cell as shown schematically in Fig. 2(a). The electrolytic cell is a quartz tube ($\phi_{in} 24 \text{ mm} \times \phi_{out} 28 \text{ mm} \times 170 \text{ mm}$) with a curved branch tube and a PTFE lid. The branch tube ($\phi_{out} 10 \text{ mm} \times 55 \text{ mm}$) for the evolved gas outlet is at the height of 10 cm from the bottom of the cell. The anode and its leads are a Pt wire of $\phi 0.5 \text{ mm} \times 1.4 \text{ m}$ (99.95%, GRINM, Beijing). The cathode is Pd as listed in Table 1 or Pt foil of $\sim 3.4 \text{ cm}^2$ (99.95%, GRINM, Beijing). The cathode lead is a Pt wire of $\phi 1.1 \text{ mm} \times 18 \text{ cm}$ (99.99%, Grikin, Beijing). All Pt leads are covered with PTFE heat shrinkable tubes to prevent catalyzing $D_2 + O_2$ recombination. D₂O (99.8at.%) is from J&K Chemical. Li₂O (Alfa Aesar, 99.5% purity) powder is dissolved in heavy water to make LiOD solution just before each electrolysis. An injection pipe made of stainless-steel is used for heavy water addition. Four different O-rings (not all shown here) are used around the lid, the two leads and the pipe to prevent gas from escaping from the lid. A short PTFE tube is used on the bottom to separate the spiral anode from the cathode. A K-type thermocouple is attached on the bottom of the cell to measure temperature (T_{bottom}).

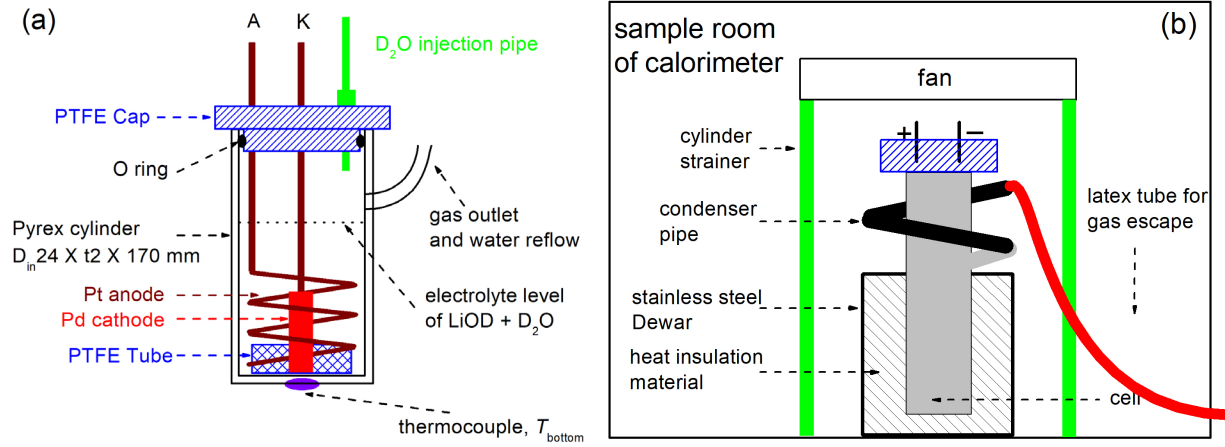


Figure 2. Schematics of Pd-D₂O reflux open-electrolytic cell (a) and the cell with calorimetric attachment (b).

The electrolytic-cell is placed in the center of a stainless-steel Dewar ($\phi_{in} 75 \text{ mm} \times \phi_{out} 83 \text{ mm} \times h_{in} 103 \text{ mm} \times h_{out} 120 \text{ mm}$) with cotton wool between the gap as heat insulation material as shown in Figs. 2(b) and 3(a). The Dewar is placed in the center of a cylinder strainer ($\phi 12 \text{ cm} \times 23 \text{ cm}$), which is covered with a fan blowing the air downward to ensure even temperature distribution in the sample chamber of the SEC as shown in Figs. 2(b) and 3(b). To make the heavy water vapor condense, a fluorine rubber tube ($\phi_{in} 10 \text{ mm} \times \phi_{out} 14 \text{ mm} \times 50 \text{ cm}$) is connected to the branch tube of the cell at one end and a 150 cm long latex tube at another end through a short glass tube as shown in Fig. 3(a). A K-type thermocouple is attached onto the short glass tube to monitor the temperature of the exit (T_{exit}) for some cases. The latex tube is extended out of the calorimeter to prevent condensation of heavy water in the sample chamber of the SEC. Gases produced in electrolysis, including oxygen, deuterium and vapor of heavy water, all escape through the outlet tube.

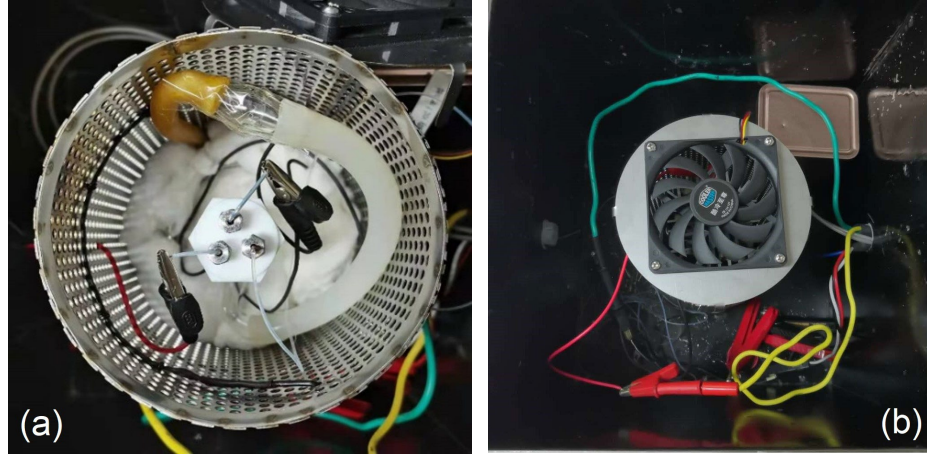


Figure 3. Photos of electrolytic cell with heat insulation (a) and fan (b) in the calorimeter.

To replenish heavy water consumed by electrolysis and evaporation, a syringe pump with injector is used to add heavy water to the cell through a PTFE tube, as shown in Figs. 2(a), 3(a) and 4. Two mode syringe pumps were used. Before Jan. 7, 2021 (Exp. #210105), Longer Pump with only simple injection function was used as shown in Fig. 4(a). From that time (Exp. #210107), Harvard Apparatus Pump 11 Elite with program function was used as shown in Fig. 4(b).



Figure 4. The syringe pumps before (a) and from (b) Jan. 7, 2021, respectively.

2.2. Calorimetry of reflux open-electrolysis

The excess power P_{ex} in the D₂O reflux open-electrolytic cell shown in Figs. 2 and 3 under steady state (input power is stable, i.e., $dP_{in}/dt = 0$) can be expressed as:

$$P_{ex} = P_{SEC} + P_{vapor} - (V_{cell} - V_{th})I \quad (1)$$

where P_{SEC} is the thermal power measured by the SEC; V_{cell} is the cell voltage; $V_{th} = 1.52666$ V at 25°C (the circulating bath of the SEC is set as $25 \pm 0.01^\circ\text{C}$), the thermoneutral potential of heavy water ($V_{th} = 1.48121$ V for light water at 25°C); I is the electrolysis current; P_{vapor} is the evaporation power, and it can be expressed as:

$$P_{vapor} = 0.75 \frac{I}{F} \frac{p}{p^* - p} L_{D_2O} \quad (2a)$$

$$= 0.00979I \text{ @ } 25^\circ\text{C} \quad (2b)$$

where F is the Faraday constant; p^* is the atmosphere pressure ($= 1.01325$ bar); $L_{D_2O} = 45.402$ kJ/mol, the evaporation enthalpy of heavy water at 25°C; $p = 0.02735$ bar, the evaporation pressure at 25°C. Because p is a small value at room temperature, therefore P_{vapor} does not change prominently with p^* as in the F-P-M situation. For light water, the constant coefficient in Eq. (2b) is 0.01104 V at 25°C.

Similarly, the rate of mass loss of heavy water in g/s during electrolysis includes contributions of electrolysis decomposition and evaporation too:

$$-\frac{dm_{D_2O}}{dt} = 0.5 \frac{I}{F} M_{D_2O} + 0.75 \frac{I}{F} \frac{p}{p^* - p} M_{D_2O} \quad (3a)$$

$$= 1.03785 \times 10^{-4} I + 4.3187 \times 10^{-6} I = 1.081 \times 10^{-4} I \text{ at } 25^\circ\text{C} \quad (3b)$$

where $M_{D_2O} = 20.0275$ g, the molecular weight of heavy water. The evaporation loss is 4.16% of the electrolysis decomposition (or 96% and 4% of total mass loss are due to Faraday process and evaporation, respectively).

For light water, the mass loss rate in g/s is:

$$-\frac{dm_{H_2O}}{dt} = 9.33576 \times 10^{-5} I + 4.52245 \times 10^{-6} I = 9.78801 \times 10^{-5} I \text{ at } 25^\circ\text{C} \quad (3c)$$

where $M_{H_2O} = 18.015268$ g, the molecular weight of light water. The evaporation loss is 4.84% of the electrolysis decomposition. In other words, 95.38% and 4.62% of total mass loss are due to electrochemical process and evaporation, respectively.

In contrast to the situation with F-P-M, atmospheric pressure p^* has little effect on power balance in Eq. (2) and mass balance in Eq. (3). We can estimate the variation range of p^* and its effect on calorimetry. Beijing's extreme atmosphere pressure is 0.9986 and 1.0204 bar in summer and winter, respectively, i.e., its simple average is 1.0095 ± 0.0109 bar (1.1%). On the other hand, the altitude of our lab's site is 59 m. The height of the SEC on the 5th floor from ground is 16 m, this means the SEC's altitude is 75 m and standard pressure should be $1.01325 \text{ bar} - 0.000112 \text{ bar/m} \times 75 \text{ m} = 1.00485 \text{ bar}$. Taking into account the above observations, the pressure in the lab should be 1.00485 ± 0.0109 bar (1.1%). For power balance, this means $P_{\text{vapor}} = (0.00987 \pm 0.00011)I$, which departs from Eq. (2) by $(0.8 \pm 1.1) \times 10^{-4} I$. For our experiments here, this correction is $59 \pm 77 \mu\text{W}$ when $I = 0.7$ A. For mass balance, the evaporation rate is $(4.3558 \pm 0.0492) \times 10^{-6} I$, which departs from the evaporation term in Eq. (3) by $(3.71 \pm 4.92) \times 10^{-8} I$. This means the correction is $(0.6 \pm 0.8)\%$ to the ideal mass loss of evaporation. These crude estimations verify that variation of atmosphere pressure cannot affect prominently our calorimetry of D₂O reflux open-electrolysis.

In electrolysis with Pd cathode, the D₂(H₂) evolution in the beginning of electrolysis is less than the ideal value in Eq. (3) due to absorption of deuterium (hydrogen) by the cathode and the D₂(H₂) evolution continues for a while after electrolysis due to desorption of deuterium (hydrogen) by palladium. However, this delay of gas evolution does not affect the steady state power balance and the total heat measurement.

Eqs. (1) and (2) are the basis of the calorimetry here. P_{vapor} is included in the output and excess power in the software. In experiments, the electrolytic-cell with the fluororubber tube and glass connector was weighed before and after each electrolysis to estimate the mass loss and check the validity of Eq. (3) and hence Eqs. (1) and (2) as listed in Table 3. It is shown that the extra D₂O losses caused by evaporation (m_{ex} , supposing the Faraday efficiency is 100%) depart from the theoretical value (m_V) by -58% to $+70\%$ in early experiments (Exp. #201004 to 201203). From Exp. #210318, a high precision balance (Ohaus PX224ZH) was used to weigh the cell, the actual mass loss was almost equal to the theoretical value under ideal conditions (e.g., $m_X/m_V = -4\%$ in Exp. #210327). Our results indicate that only the D₂O evaporation at ambient temperature but not cell temperature needs to be considered for reflux open-electrolytic cell. The maximum temperature increment of the short glass connector (see Fig. 3(a)) between the

fluororubber tube and latex tube during electrolysis was 2.61°C when the cell bottom temperature (T_{bottom}) was 96°C (D₂O vapor pressure is 0.83 bar at this temperature) in Exp. #200713 for Pt-D₂O system (see Table 4 below). This also verifies the vapor is cooled to around ambient temperature through 50 cm length of condensing tube. Because there is another 50 cm of latex tube for D₂O condensing in the sample chamber of the SEC, there is no doubt about the validity of Eqs. (1) to (3) although the mass losses are not exactly the same as the theoretical prediction as listed in Table 3 sometimes, due to two reasons: (1) the fluororubber tube should be replaced with glass tube because the former is hygroscopic and its moisture content changes before and after electrolysis; (2) the quantity of D₂O addition was not measured precisely in these experiments.

Table 3. Theoretical and actual D₂O losses during electrolysis and related corrections to excess power measurement.

Exp. #	T_{bottom} °C	m_E g	m_V g	m_T g	m_A g	m_{ex} g	R %	P_C mW	P_{ex} mW
201004	97	6.26	0.26	6.52	6.61	0.09	35	2	-28
201006	97	14.78	0.61	15.40	15.42	0.02	4	0.2	-18
201009									59
201021	97	8.83	0.37	9.20	8.98	-0.21	-58	-4	-3
201127	96	8.38	0.35	8.73	8.97	0.24	70	3	-94
201203	82	4.61	0.19	4.80	4.76	-0.03	-18	-1	-51
210318	75-82	9.4471	0.3931	9.8402	9.7806	0.3335	85	6	7
210322	83-85	6.3081	0.2625	6.5706	6.6484	0.0779	30	2	NA
210327	73-80	11.8443	0.4929	12.3372	12.3184	-0.0188	-4	0	NA
210511Pt	NA	7.6586	0.3420	8.0006	7.9654	-0.0352	-10	0.2	-8
210517Pt	NA	7.6486	0.3494	7.9980	7.8986	-0.0994	-28	-0.5	3
210520Pt	35-79	7.6488	0.3494	7.9982	7.9517	-0.0465	-13	-1	24
210526Pt	37-87	7.6586	0.3588	8.0071	7.9133	-0.0938	-26	-0.5	29
210529Pt	40-90	5.5653	0.2705	5.8358	5.7431	-0.0927	-34	-1	29

* Meanings of symbols: m_E , D₂O loss by direct electrolysis; m_V , D₂O loss by evaporation at 25°C; $m_T = m_E + m_V$, theoretical value of D₂O loss during electrolysis; m_A , actual D₂O loss through weighting before and after electrolysis and addition of D₂O; $m_{\text{ex}} = m_A - m_T$, extra value of D₂O loss; $R = m_{\text{ex}}/m_V$, correction factor; P_C , correction of excess power assuming that the extra mass loss is induced by evaporation of D₂O; P_{ex} , excess power measured by SEC.

* Density of heavy water is 1.10436 g/ml at 25°C [13].

In a word, the reflux open-electrolytic cell is an effective design to reduce the evaporation process' influence on power balance, which was the biggest uncertainty omitted or debated in calorimetry of open electrolysis in the past cold fusion works [5-8]. We hope this design can put an end to this dispute.

In our experiments, the cell voltage and current, temperatures and calorimetric signals are all recorded in real-time by a computer every second. The calorimeter is calibrated every month to ensure accuracy.

3. Results and discussions

3.1. Improvement of calorimetry

Over the last three years, a new technique, namely convolution-denoising, for the SEC was developed in our lab ^[14]. Its principle is as follows: in the light that the thermal power noise of the SEC mainly comes from temperature fluctuations of cooling fluid, our goal is to measure the fluctuation and eliminate it. Here is the solution: a reference cell, which is much smaller than the SEC, is placed between the outlet of the constant temperature bath and the sample cell (i.e., in the main part of the SEC) (Fig. 5). This design ensures that any change of thermal signal of the reference cell induced by the fluctuation of fluid temperature occurs prior to the response of sample cell. Before routine calorimetry is performed, a temperature pulse is applied on purpose to induce two thermal pulses in the reference cell and sample cell to occur successively. Then by deconvoluting these two pulses, the response function can be obtained. In routine calorimetry, the convolution waveform of thermal signal of the reference cell is much like the signal of the sample cell induced by the fluid temperature fluctuation. Taking the difference between them can eliminate most of thermal noise, as shown in Fig. 6(a). An example of the calibration in Exp. #210315 using the convolution-denoising technique is shown in Fig. 6(b), the standard deviation is only 1.3 mW this time and is one order smaller than before ^[12]. This technique ensures that the sensitivity and accuracy of decimeter-size-sampled SEC can approach the levels of IPC of F-P-M ^[2,5-8].

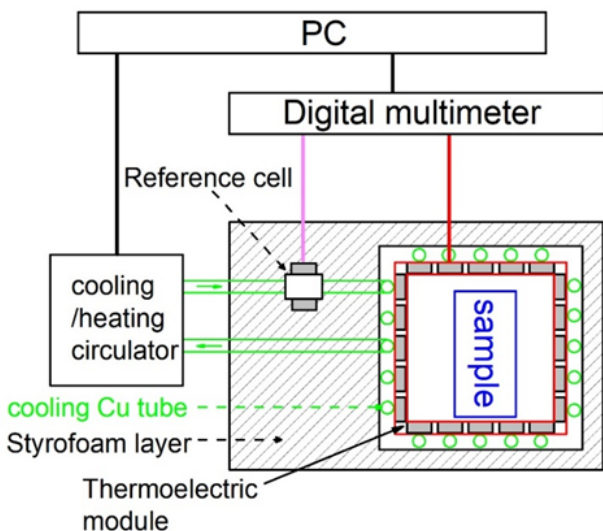


Figure 5. Position of reference cell between constant temperature bath and cell.

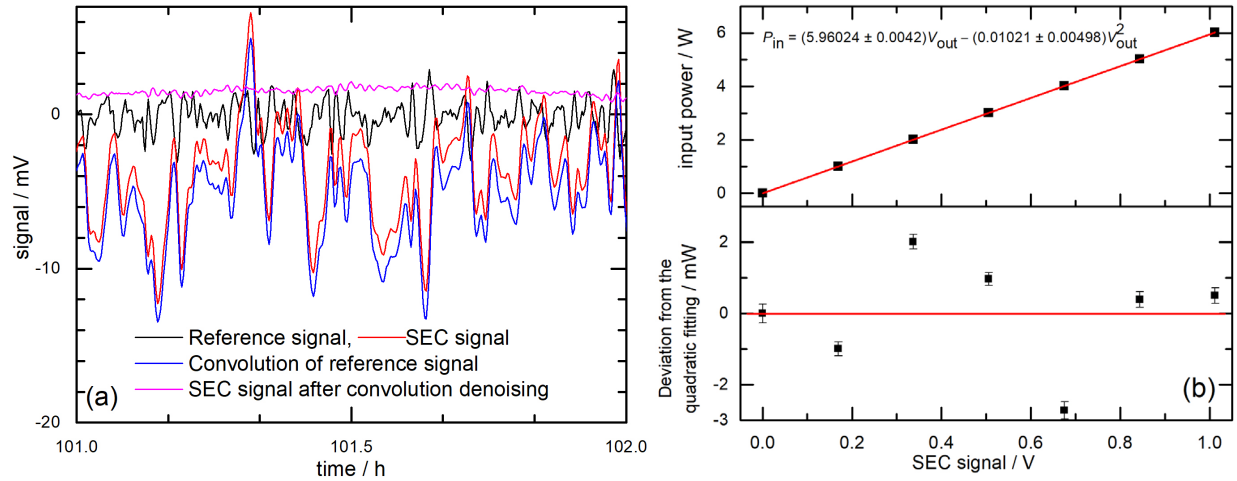


Figure 6. (a) One example of denoising technique; (b) Calibration results of SEC with an electric heater at 25°C in Exp. #210315.

3.2. Calorimetric results of Pt-D₂O(H₂O) reflux open-electrolytic cells

The Pt-D₂O reflux open-electrolytic cell and its assembly in the SEC are shown in Fig. 7. Examples of excess heat in Pt-D₂O and Pt-H₂O systems are shown in Fig. 8. Calorimetric results of 18 runs electrolysis of D₂O and 3 runs of H₂O are summarized in Tables 4 and 5, respectively. Excess power that varies with current, input power and temperature listed in Tables 4 and 5 is graphically represented in Fig. 9.

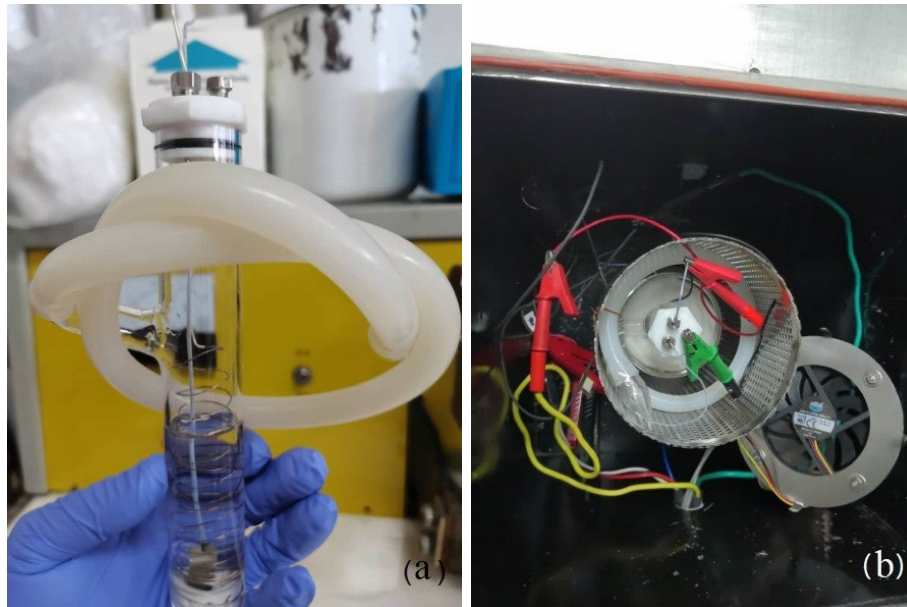


Figure 7. Photos of the Pt-D₂O open cell used in experiments (a) and the cell in the calorimeter (b).

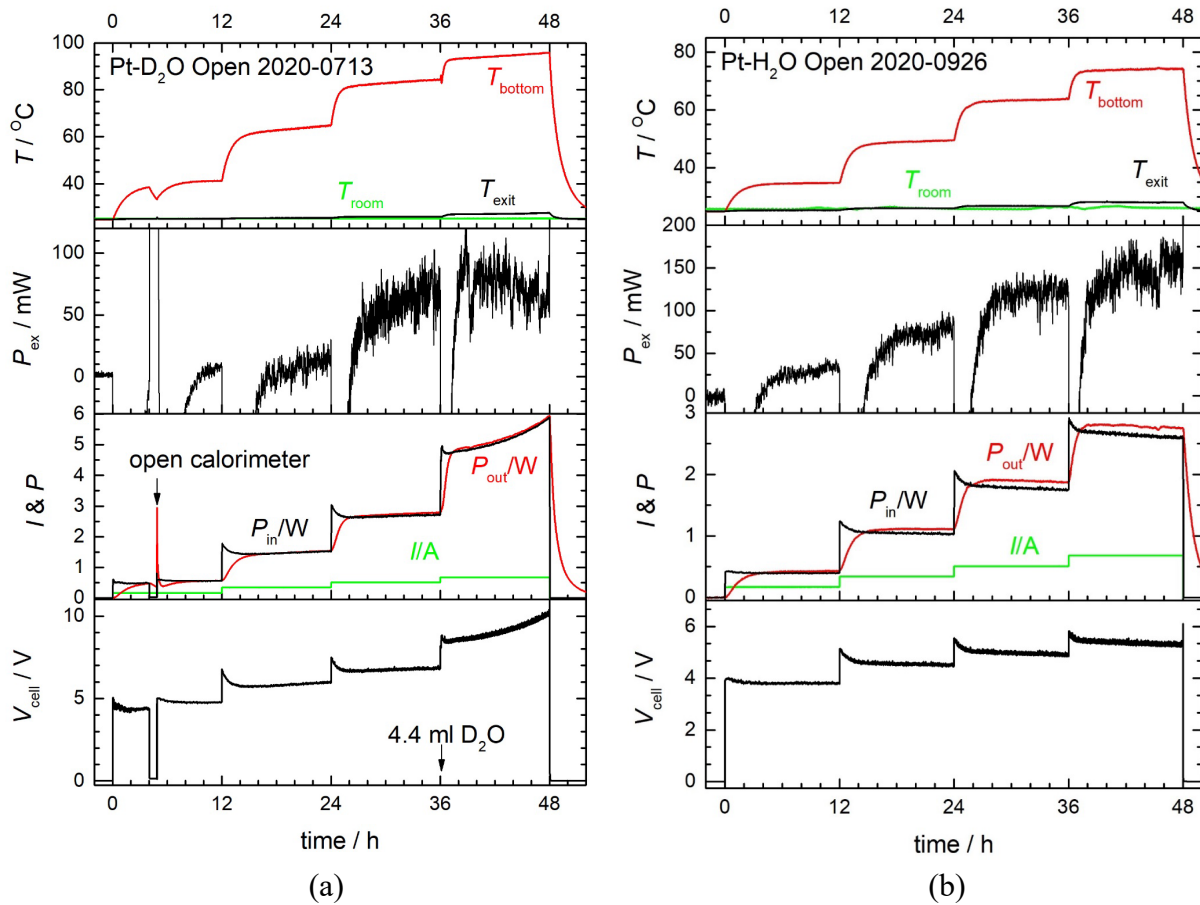


Figure 8. Examples of excess power in open-electrolytic Pt-D₂O (a) and Pt-H₂O (b) cells. The physical quantities in this figure are cell voltage (V_{cell}), electrolysis current (I), input power (P_{in}), output power (P_{out}), excess power (P_{ex}), room temperature (T_{room}) and cell-bottom temperature (T_{bottom}). Other related information is listed in Tables 4 and 5, respectively.

Table 4. Summary of excess heat in Pt-D₂O+LiOD reflux open-electrolytic cell from 2020 to 2021.

Cal. #	Exp. #	$I \times t$ Ah	Integrated values			Steady values				
			Q_{in} kJ	Q_{ex} kJ	\bar{P}_{ex} mW	I mA	dP_{in}/dt mW/h	P_{in} W	P_{ex} mW	T_{bottom} °C
200618	200619Pt1	0.17×24, 0.34×10, 0.51×10, 0.68×10	236.28(14)	4.16(66)	21(3)	169	0.45	0.404(2)	13(3)	34
						339	−1.3	1.069(6)	18(10)	46
						509	−6.9	1.811(10)	28(8)	58
						679	−15	2.592(22)	48(12)	68
	200626Pt1	0.17×6, 0.34×6, 0.51×6, 0.68×6, 0.85×5	SEC signal was unstable after electrolysis			170	−0.83	0.383(2)	−3(2)	35
						340	0.50	1.017(3)	5(4)	51
						510	−4.6	1.749(6)	14(6)	65
						680	−6.3	2.583(8)	31(7)	76
						850	7.7	3.475(8)	38(11)	84
200629	200701Pt1	0.17×12, 0.34×12, 0.51×6.5	Calorimetry interrupted due to malfunction			170	2.7	0.434(2)	13(3)	36
						340	−6.9	1.125(4)	37(4)	53
	200703Pt1	0.17×12, 0.34×12, 0.51×12, 0.68×12, 0.85×12	459.95(11)	1.84(111)	8(5)	170	0.99	0.425(3)	5(3)	37
						341	−1.5	1.102(5)	15(5)	54
						511	−10	1.993(8)	23(8)	68
						681	−14	2.875(12)	34(9)	80
						851	31	4.239(20)	−8(14)	91
200708	200713Pt1	0.17×12, 0.34×12, 0.51×12, 0.68×12	423.49(11)	10.16(127)	59(7)	171	−1.1	0.554(2)	6(3)	41
						341	11	1.516(8)	13(6)	64
						511	9.3	2.711(14)	69(14)	84
						681	174	5.685(11)	64(11)	96
	200908Pt1	0.17×12, 0.34×12, 0.51×12, 0.68×12, 0.85×12	460.36(10)	7.02(76)	28(3)	170	0.28	0.409(1)	6(2)	35
						340	−2.0	1.083(4)	20(5)	50
						510	−9.5	1.861(8)	43(8)	65
						680	−11	2.984(14)	68(16)	76
						850	−6.1	4.139(12)	79(12)	87
200916	200912Pt2	0.17×12, 0.34×12, 0.51×12, 0.68×12, 0.85×12	487.76(10)	3.87(76)	15(3)	170	−1.2	0.450(2)	11(10)	36
						340	−4.2	1.126(3)	16(4)	52
						510	−7.7	1.854(4)	35(4)	66
						680	−3.2	2.818(5)	42(5)	80
						850	31	5.178(53)	23(27)	92
	200918Pt2	0.17×12, 0.34×12, 0.51×12, 0.68×12, 0.85×12	569.92(12)	6.51(157)	26(6)	170	−0.63	0.471(4)	12(5)	37
						340	−2.0	1.226(12)	37(14)	54
						510	−5.8	2.114(16)	57(17)	71
						680	6.2	3.490(69)	53(58)	86
						850	31	6.183(75)	10(54)	95
200922Pt2	200922Pt2	0.17×12, 0.34×12, 0.51×12, 0.68×12, 0.85×12	831.14(17)	−0.27(162)	−1(7)	170	0.0013	0.650(4)	36(5)	40
						340	1.7	1.760(23)	46(22)	61
						510	16	2.851(90)	44(63)	80

						680	21	4.887(93)	16(67)	92
						850	433	11.179(312)	-376(76)	98
						521		2.003(11)	12(12)	64
						848		4.008(47)	9(52)	87
						1053	0	6.017(82)	-22(96)	95
201016Pt3	2, 4, 6, 8, 10 W each for 9 h	Originally calibrating SEC				1092		8.002(149)	-73(164)	96
						1150		10.004(130)	-119(132)	97
						283		1.004(1)	3(2)	
						470		2.016(2)	15(49)	
						623	0	3.008(70)	42(70)	NA
201125Pt4	1, 2, 3, 4, 5 W each for 8 h	ib id				733		4.003(99)	42(100)	
						778		5.004(123)	14(124)	
						356		1.201(12)	8(13)	
						605		2.402(21)	30(21)	
						796	0	3.603(35)	44(36)	NA
201206Pt4	1.2, 2.4, 3.6, 4.8, 6 W each for 8 h	ib id				904		4.809(78)	40(87)	
						978		6.012(57)	28(59)	
						286		1.004(12)	-6(20)	49
						447		2.011(91)	-2(100)	65
						598		3.011(77)	72(87)	78
210126Pt4	1, 2, 3, 4, 5, 6 W each for 8 h	ib id				741	0	4.014(103)	95(113)	88
						827		4.998(100)	62(106)	93
						855		6.026(112)	45(121)	96
						171	-0.87	0.453(3)	-7(6)	
						341	-3.1	1.170(8)	5(12)	NA
210508	210511Pt4	0.17×12, 0.34×12, 0.51×12, 0.68×12	295.40(7)	-1.33(70)	-8(4)	512	-1.4	2.057(15)	5(18)	
						681	3.8	3.013(12)	-18(17)	
						171	0.12	0.513(3)	1(3)	
						341	-3.9	1.306(11)	8(11)	NA
						511	33	2.243(16)	9(15)	
210515	210517Pt4	0.17×12, 0.34×12, 0.51×12, 0.68×12	320.53(7)	0.48(46)	3(3)	681	8.3	3.314(21)	4(20)	
						171	-0.72	0.462(4)	5(5)	36
						341	-3.8	1.163(7)	24(8)	50
						511	-8	1.910(11)	40(11)	65
						681	20	3.051(20)	30(13)	79
210515	210520Pt5	0.17×12, 0.34×12, 0.51×12, 0.68×12	286.71(7)	4.06(46)	24(3)	171	0.36	0.546(5)	12(6)	37
						341	-2.6	1.389(10)	20(10)	55
						511	-9.4	2.360(17)	44(17)	71
						681	98	4.001(131)	8(24)	87
						171	-0.04	0.635(6)	2(6)	40
210515	210526Pt5	0.17×12, 0.34×12, 0.51×12, 0.68×12	353.29(8)	4.85(46)	29(3)	341	-0.49	1.573(9)	32(9)	60
						511	51	3.068(56)	16(31)	79

*Sizes and masses of Pt cathode: (1) Pt#1 in Exp. #200619 to 200908, $5.5 \times 31 \times 0.02 \text{ mm}^3$, 3.4 cm^2 , $70.0(1) \text{ mg}$; (2) Pt#2 in Exp. #200912 to 201009, $7.4 \times 23 \times 0.02 \text{ mm}^3$, 3.4 cm^2 , $65.9(1) \text{ mg}$; (3) Pt#3 in Exp. #201013 to 201016, $7.30 \times 23.56 \times 0.02 \text{ mm}^3$, 3.4 cm^2 , $72.2(2) \text{ mg}$; (4) Pt#4 in Exp. #201125 to 2010126, $7.36 \times 22.52 \times 0.02 \text{ mm}^3$, 3.3 cm^2 , $67.7(1) \text{ mg}$; (5) Pt#5 in Exp. #201517 to 210526, $7.5 \times 22 \times 0.02 \text{ mm}^3$, 3.4 cm^2 , $66.6(3) \text{ mg}$.

Table 5. Summary of excess heat in Pt-H₂O+LiOH reflux open-electrolytic cell from 2020 to 2021.

Cal#	Exp. #	Integrated values				Steady values				
		$I \times t$ A × h	Q_{in} kJ	Q_{ex} kJ	\bar{P}_{ex} mW	I mA	dP_{in}/dt mW/h	P_{in} W	P_{ex} mW	T_{bottom} °C
200916	200926Pt2	0.17×12, 0.34×12, 0.51×12, 0.68×12	255.69(7)	15.47(52)	90(3)	171	0.038	0.397(1)	34(4)	35
						341	−0.3	1.034(7)	79(8)	49
						511	−6.8	1.755(9)	123(10)	64
						681	−10	2.606(12)	156(12)	74
210515	210601Pt5	0.17×12, 0.34×12, 0.51×12, 0.68×12	239.73(6)	1.75(44)	10(3)	172	0.22	0.369(1)	−1(3)	34
						342	−2.2	0.974(3)	13(4)	47
						512	−6.0	1.674(6)	21(7)	60
						682	−16	2.409(25)	27(24)	72
	210604Pt5	0.17×12, 0.34×12, 0.51×12, 0.68×12	259.57(6)	4.60(46)	27(3)	172	−0.43	0.404(1)	4(3)	34
						342	−3.8	1.014(5)	34(4)	51
						512	5.1	1.868(52)	30(44)	62
						682	−18	2.631(83)	57(52)	75

* Sizes and masses of Pt cathode are the same as that in Table 4.

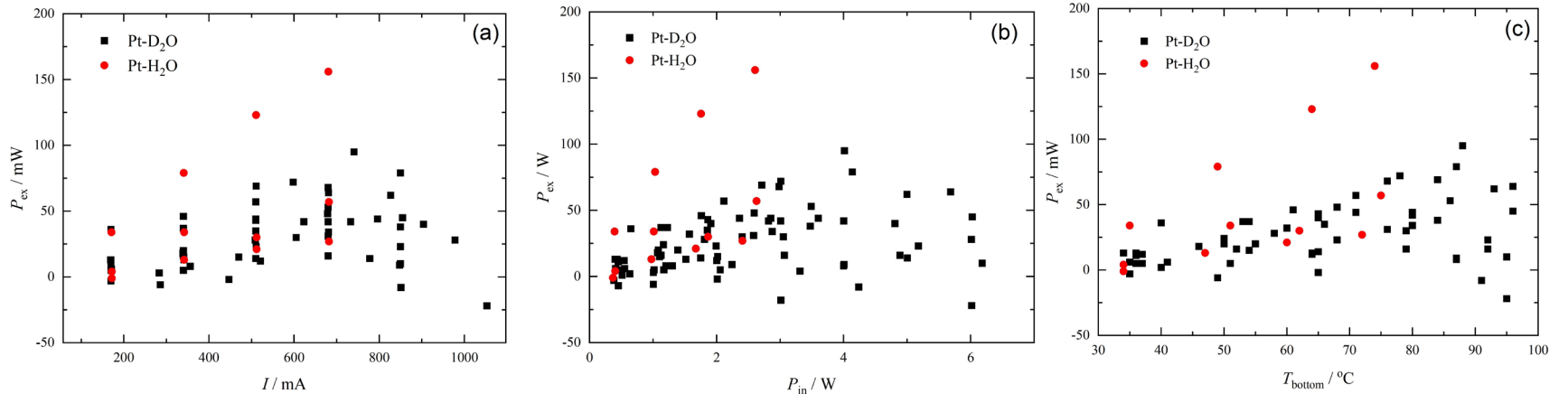


Figure 9. Excess power in Pt-D₂O(H₂O) reflux open-electrolytic cell from 2020 to 2021.

Originally, the Pt-D₂O(H₂O) cell was used as the control system to verify the validity of calorimetry from June to Sep. 2020 (Exp. #200619 to 200922). However, it was found the Pt-D₂O(H₂O) cell always produced excess heat, and the Pd-D₂O cell did not always give positive results in these runs. We thought there must be a heat distribution error between the Pt-D₂O system and the calibration heater. So, from Exp. #201016 to 210126, we used the Pt-D₂O cell to calibrate the SEC. Because the constant power mode was applied in these runs, $dP_{in}/dt = 0$ was satisfied through the control of current by software as listed in Table 4. During these runs, the data logging was stopped after the output signal of the SEC became stable, therefore total heat was not measured. After that, we realized that the excess heat was indeed produced in the Pt-D₂O(H₂O) cell, and its calorimetric procedure being similar to that of Pd-D₂O system was applied intentionally from Exp. #210511 to 210604. We can find that most of Pt-D₂O(H₂O) open-electrolytic cells exhibited prominent excess power (> 30 mW) while $I > 0.5$ A and light water electrolysis gave about 2 times the excess power of heavy water systems at the same input power, as listed in Tables 4 and 5 and shown in Fig. 9. The maximum average excess power is 59 ± 7 mW with average input power of 2.5 W (~ 423.49 kJ/48 h) in Exp. #200713 for Pt-D₂O system and 90 ± 3 mW with average input power of 1.5 W (~ 255.69 kJ/48 h) in Exp. #200926 for Pt-H₂O system.

For Pt-D₂O systems, although the total excess heat is -0.27 ± 1.62 kJ ($\bar{P}_{ex} = -1 \pm 7$ mW) in Exp. #200922 and it looks like that this run is a perfect control experiment. However, this is just a coincidence because the instantaneous value of excess power is positive in stable electrolysis and negative excess power is always observed in unstable electrolysis, as will be discussed afterwards. This means that the zero value of excess heat is just the result of positive and negative values offsetting each other.

Dash^[15] and Lonchamp et al.^[16] also reported excess heat in Pt-D₂O electrolysis system before; however, where the heat comes from still remains to be determined.

3.3. Calorimetric results of Pd-D₂O reflux open electrolytic cells

Calorimetric results of open-electrolytic system with Pd#3 are summarized in Table 6. The electrolytic cell with this cathode and the sample after long duration electrolysis is shown in Fig. 10. An example of calorimetry is shown in Fig. 11. Two runs with Pd #3, Exp. #201002 and 201209, produced excess heat. The sample was covered with a black deposition after long duration electrolysis, as shown in the electrode image of Fig. 10(b). After ultrasonic cleaning in water, the deposition fell off, and it was found to be lithium silicate (Li₂SiO₃) as sediment on the bottom, as verified in Section 3.5.

Table 6. Summary of excess heat in Pd#3-D₂O+LiOD reflux open-electrolytic cell.

Exp. #	$I \times t$ A \times h	Integrated values			period h	dP_{in}/dt mW/h	Steady values		
		Q_{in} kJ	Q_{ex} kJ	\bar{P}_{ex} mW			P_{in} W	P_{ex} mW	T_{bottom} °C
200929	0.68 \times 24	309.74(6)	-0.36(81)	-4(9)	12-14	-7.1	3.586(19)	18(19)	84
					22-24	-11	3.349(18)	25(19)	85
201002	0.75 \times 24	352.20(7)	1.60(81)	19(9)	12-14	1.7	3.995(16)	41(15)	87
					22-24	17	4.188(14)	32(12)	90
201004	0.85 \times 24	631.97(12)	-6.41(81)	-74(9)	10-12	17	6.890(106)	-80(22)	96
					22-24	363	9.397(242)	-181(35)	97
201006	0.80 \times 24	500.26(9)	-0.35(81)	-4(9)	10-12	56	5.763(34)	-3(13)	93
					22-24	14	6.359(34)	14(28)	96
201009	0.8 \times 29,0.6 \times 11	1280.02(24)	-11.40(119)	-79(8)	6-8	169	7.496(131)	-46(56)	95
201021	0.80 \times 36	1024.26(19)	-11.86(109)	-92(8)	10-12	36	7.110(155)	-70(44)	97
201127	0.5 \times 52	994.00(21)	-17.93(153)	-90(8)	10-12	41	4.061(22)	-48(18)	91
201203	0.5 \times 30	325.75(7)	-2.51(94)	-23(9)	28-30	5.6	3.061(16)	-22(13)	84
					20-24	-7.2	3.048(18)	33(16)	84
201209	0.5 \times 102	NA	NA	NA	58-62	-10	3.379(27)	36(25)	88
					82-86	33	3.837(44)	11(25)	90

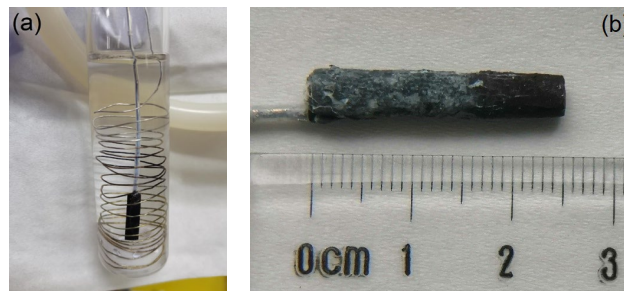


Figure 10. The electrolytic cell with Pd#3 before Exp. #200929 (a) and Pd#3 after Exp. #201203 (b).

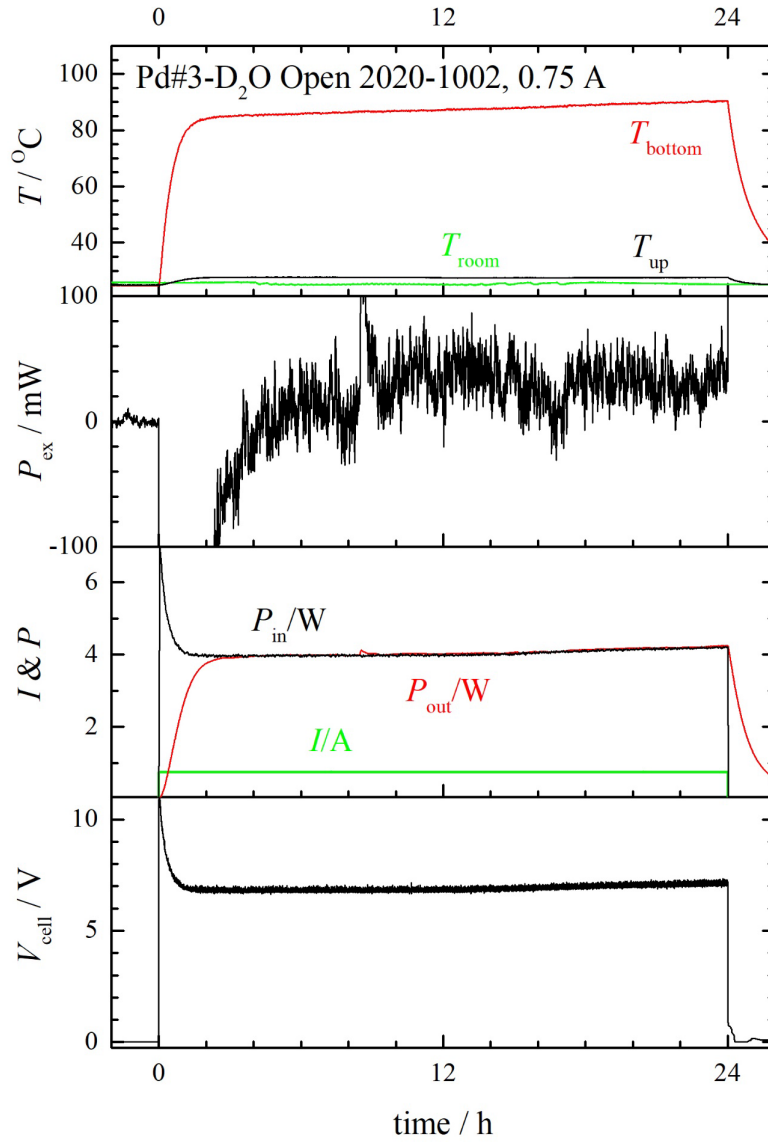


Figure 11. Electrochemical and calorimetric parameters in electrolysis of Pd#3-D₂O in Exp. #201002.

Calorimetric results of open-electrolytic system with Pd#2 are summarized in Table 7. The electrolytic cell with this cathode and the sample after long duration electrolysis are shown in Fig. 12. An example of calorimetry is shown in Fig. 13.

Table 7. Summary of excess heat in Pd#2-D₂O+LiOD reflux open-electrolytic cell.

Exp. #	$I \times t$ A × h	Integrated values			period h	dP_{in}/dt mV/h	Steady values		
		Q_{in} kJ	Q_{ex} kJ	\bar{P}_{ex} mW			P_{in} W	P_{ex} mW	T_{bottom} °C
201225	0.5×12	78.99(3)	0.83(54)	19(12)	8–12	–60	1.755(121)	26(68)	58
201227	0.6×180	1229.50(25)	13.88(430)	21(7)	54–60 174–180	–6.6 –2.9	1.799(12) 1.978(10)	40(9) 26(9)	63 66
210105	0.75×24				17–20	–3.4	2.823(10)	45(11)	78
210107	0.75×72	1104.89(19)	2.58(182)	10(7)	16–20 10–12	11 –4.5	3.052(81) 3.207(9)	35(52) 17(11)	78 83
210111	0.7×60	783.00(14)	2.70(161)	12(7)	22–24 46–48	–7.6 4.1	3.347(11) 3.774(13)	30(0) 18(14)	84 87
210129	0.7×36	843.36(16)	–7.54(108)	–58(8)	16–18	53	5.715(38)	–36(23)	94
210203	0.7×60	1184.56(21)	–8.52(162)	–39(7)	10–12	12	3.513(23)	–30(25)	85
210306	0.7×36	374.15(7)	5.91(43)	46(3)	10–12	–23	2.646(101)	48(66)	74
210318	0.7×36	423.04(8)	0.87(24)	7(2)	18–20	–1.3	3.093(12)	8(12)	76



Figure 12. Pd#2 cathode and anode before first experiment of #201225 (a) and the cathode after Exp. #210111 (b).

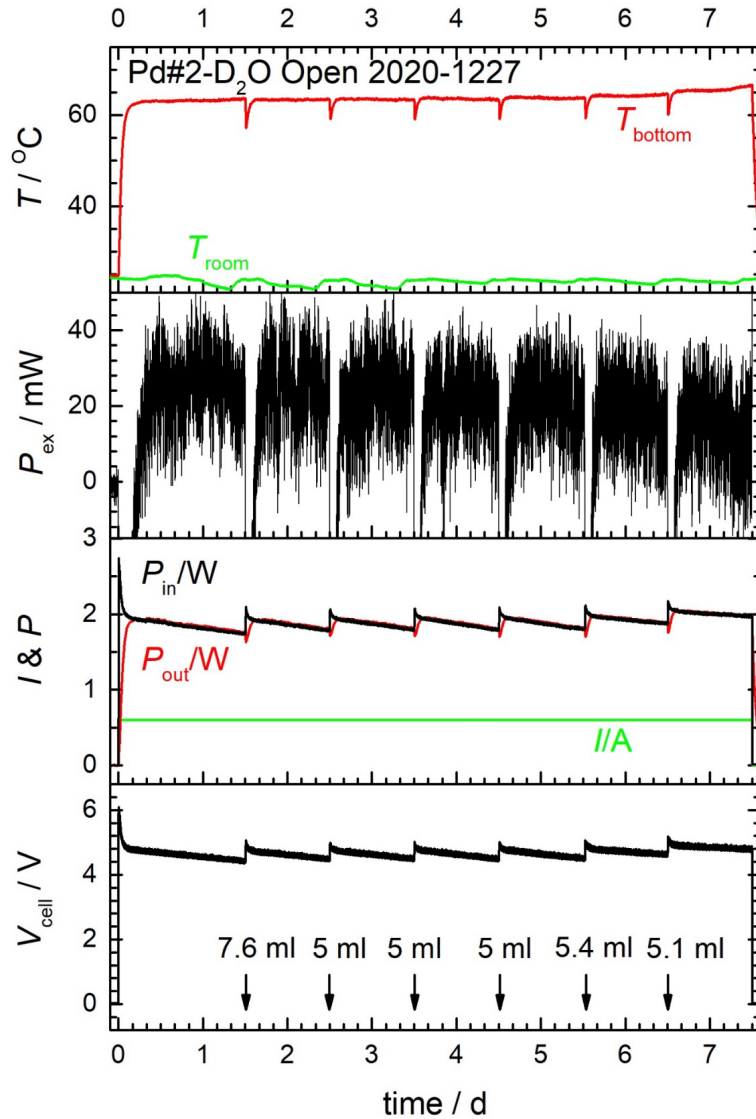


Figure 13. Electrochemical and calorimetric parameters in electrolysis of Pd#2-D₂O in Exp. #201227.

The maximum average excess power is 19 ± 9 mW with average input power of 4.1 W (~ 352.2 kJ/24 h) in Exp. 201002 for Pd#3 and 46 ± 3 mW with average input power of 2.9 W (~ 374.15 kJ/36 h) in Exp. #210306 for Pd#2. Although both two Pd cathodes exhibited activity, the amplitudes of excess heat are only in the order of ten milliwatts, which is one order lower than that reported by Miles ^[5–8], and the reproducibility is low. This is the most important problem for us.

3.4. Effects of unsteady electrolysis on calorimetry

Generally speaking, open electrolysis of D₂O is under an unsteady state as discussed by Miles previously ^[7]. In our experiments, two kinds of unsteady state are categorized according to the change rate of cell voltage V_{cell} (or input power P_{in}). The first is long-term shift (LTS) of V_{cell} or P_{in} caused by dissipation of D₂O and LiOD (or

H₂O and LiOH for a light water system), as shown in Figs. 8, 11 and 13. Another is short-term fluctuation (STF) of V_{cell} (or P_{in}) resulted from a bad electrode configuration or high current, as shown in Fig. 14 below.

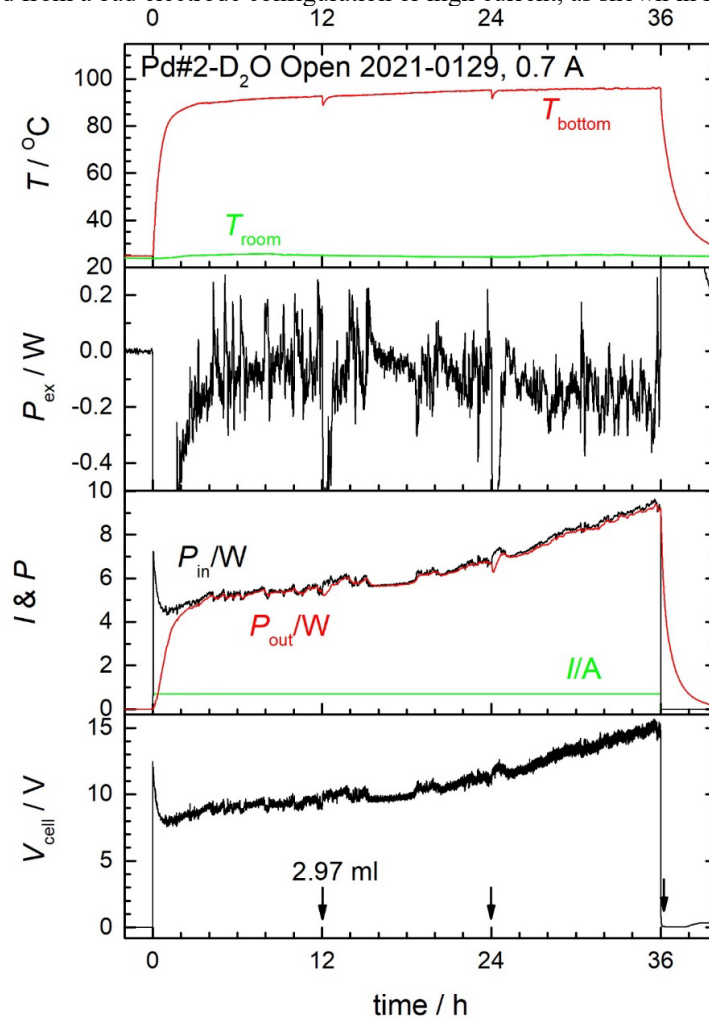


Figure 14. Electrochemical and calorimetric parameters in electrolysis of Pd#2-D₂O (Exp. #210129).

Strictly speaking, D₂O electrolysis in the present narrow space is not as stable as it is in the wide cell used by us before ^[9–12] as shown in Fig. 15. During electrolysis, gas bubbles are produced, and they grow and break on surfaces of electrodes. Along with these processes, V_{cell} and P_{in} increase to the maximum values just before the bubbles break. Fig. 15(a) shows the details of voltage changing in Fig. 13. It can be seen that V_{cell} undergoes about 2 periods of growth-break process in 3 minutes in the long-term shift (LTS) state. However, this voltage change does not affect calorimetry because the changing details of voltage and power can be recorded in real-time (data logging rate is once per second as described above).

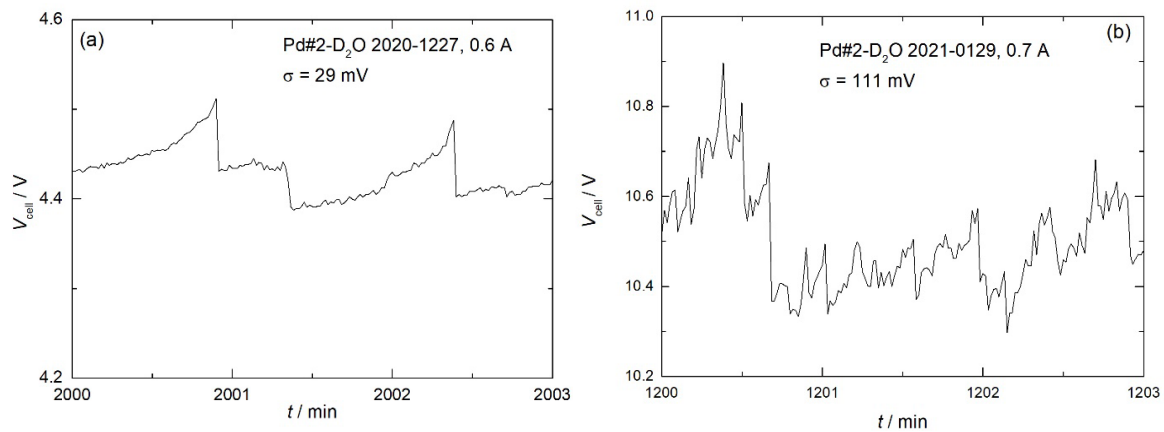


Figure 15. Characteristics of voltage variation with time in Exp. #201227 (a) and #210203 (b) for Pd#2.

As far as the LTS of input power is concerned, we found that the P_{in} decreases or increases occur every ten hours or so, depending on different current and different period as listed in Tables 4 to 7 and shown in Figs. 8, 11 and 13, therefore, the condition of $P_{in}/dt = 0$ of Eq. (1) is difficult to be satisfied. In the meantime, the positive dP_{in}/dt will induce decreasing of P_{ex} , and the negative dP_{in}/dt will induce increasing of P_{ex} correspondingly.

Two factors control the LTS of V_{cell} and P_{in} . If D₂O(H₂O) dissipation dominates the process, a concentrated solution will make the electrolyte resistance, V_{cell} and P_{in} decrease with time ($dP_{in}/dt < 0$) and P_{ex} greater than the steady state (e.g., Exp. #200926 shown in Fig. 8(b) and listed in Table 5, Exp. #201227 listed in Table 7 and shown in Fig. 13). On the other hand, the loss of LiOD makes electrolyte resistance, V_{cell} and P_{in} increase with time ($dP_{in}/dt > 0$) and P_{ex} smaller than the steady state (e.g., Exp. #200712 shown in Fig. 8(a) and listed in Table 4). If these two tendencies can be offset as far as possible, steady electrolysis can be approached (e.g., Exp. #200922 at 0.17 A listed in Table 4, Exp. #201002 listed in Table 6).

In our calorimetry, the basic standard of existence of anomalous heat is total excess heat $Q_{ex} > 2\sigma$, in the meantime the instantaneous excess power must be accompanied by dP_{in}/dt to avoid misjudgment due to the delay response of the SEC. This means that the average excess power ($= Q_{ex}/t$, the total excess heat divided by electrolysis time) differs from instantaneous values in electrolysis as listed in Tables 4 to 7. Fig. 16 shows that P_{ex} changes with dP_{in}/dt in Exp. #201227. The linear simulation gives the intercept of 18 mW, which should be the real value under steady state if the excess power did not change in electrolysis, and it is closer to the average value of 21 mW listed in Table 6 than any instantaneous value between 26 to 41 mW. This mechanism can explain the discrepancy of excess power between different methods, and also indicates that our calorimetry is reliable. Another example is Exp. #200929 for Pd#3 listed in Table 6. $P_{ex} = 18 \pm 19$ mW with $dP_{in}/dt = -7.1$ mW/h in 12 – 14 h, and $P_{ex} = 25 \pm 19$ mW with $dP_{in}/dt = -10.8$ mW/h in 22 – 24 h. Using the linear simulation similar to Fig. 16, we obtain the slope, -1.74 h⁻¹, which is in the same order as -2.93 h⁻¹ shown in Fig. 16, and the intercept is 6 mW, which is closer to the average value -4 ± 9 mW listed in Table 6 than the above instantaneous values. The extreme situation of LTS frequently occurring is that the cell voltage and input power increases prominently when the LiOD concentration is low or/and electrolytic current was high, the output power cannot follow the increase of input power and the excess power will be a prominent negative value. An extremely example is that $P_{ex} = -376$ mW while $dP_{in}/dt = 433$ mW/h at 0.85 A in Exp. #200922 for a Pt cathode listed in Table 4.

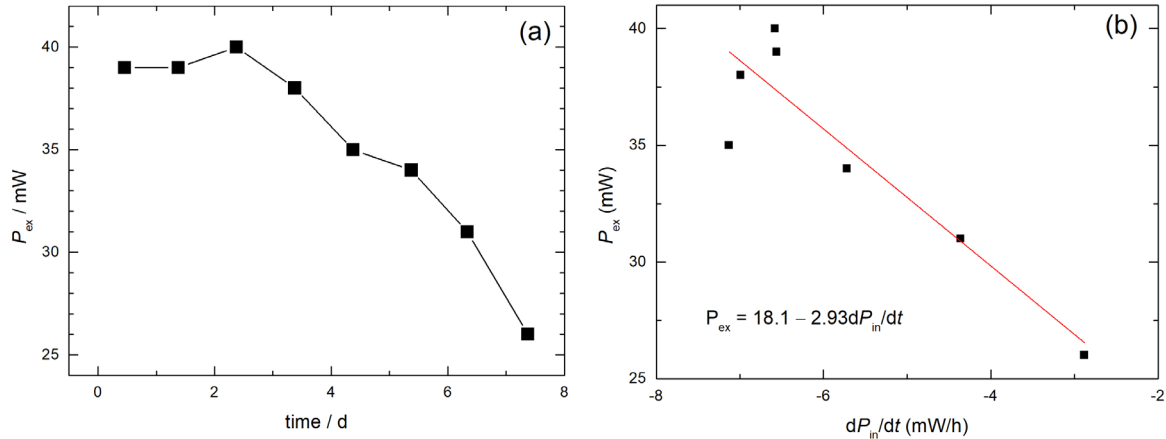


Figure 16. (a) Excess power of 6-h average P_{ex} changing with time and (b) P_{ex} vs. dP_{in}/dt in Exp. #201227 shown in Fig. 13.

The STF (short-term fluctuation) state shown in Fig. 15(b) always occurs under the following conditions: (i) the current is high (e.g., 1.15 A in Exp. #201016 in Table 4); (ii) the cathode is not in the center of the cell or is covered with deposition of Li₂SiO₃; (iii) the anode is not an ideal spiral, or the cell is not upright. More than 30 peaks occurred in 3 minutes in Fig. 15(b) and the standard deviation of average value of V_{cell} is 111 mV, 3.8 times of that in LTS state in Fig. 15(a). The data logging rate cannot follow or reflect the voltage changing in STF state, the input power is overestimated and the excess power may (not absolutely) be negative such as:

- Exp. #190904, 190920 for Pd#3 in Table 2;
- Exp. #201016 for Pt cathode in Table 4;
- Exp. #201004, 201009 and 201021 for Pd#3 in Table 6;
- Exp. #210129 and 210203 for Pd#2 in Table 7.

If the Pd electrode is active enough, the output power may exceed the overestimated input power, and excess power will still be a positive value (e.g., Exp. #210306 in Table 7).

The STF state can be avoided through better configured electrodes and appropriate current in future work. However, there are uncontrolled factors in the experiments. We find that the STF state becomes serious once in a while in Exp. #201203 shown in Fig. 17(a), and electrolysis changing from the LTS to STF state after electrolysis for 12 hours in Exp. #210203, as shown in Fig. 17(b).

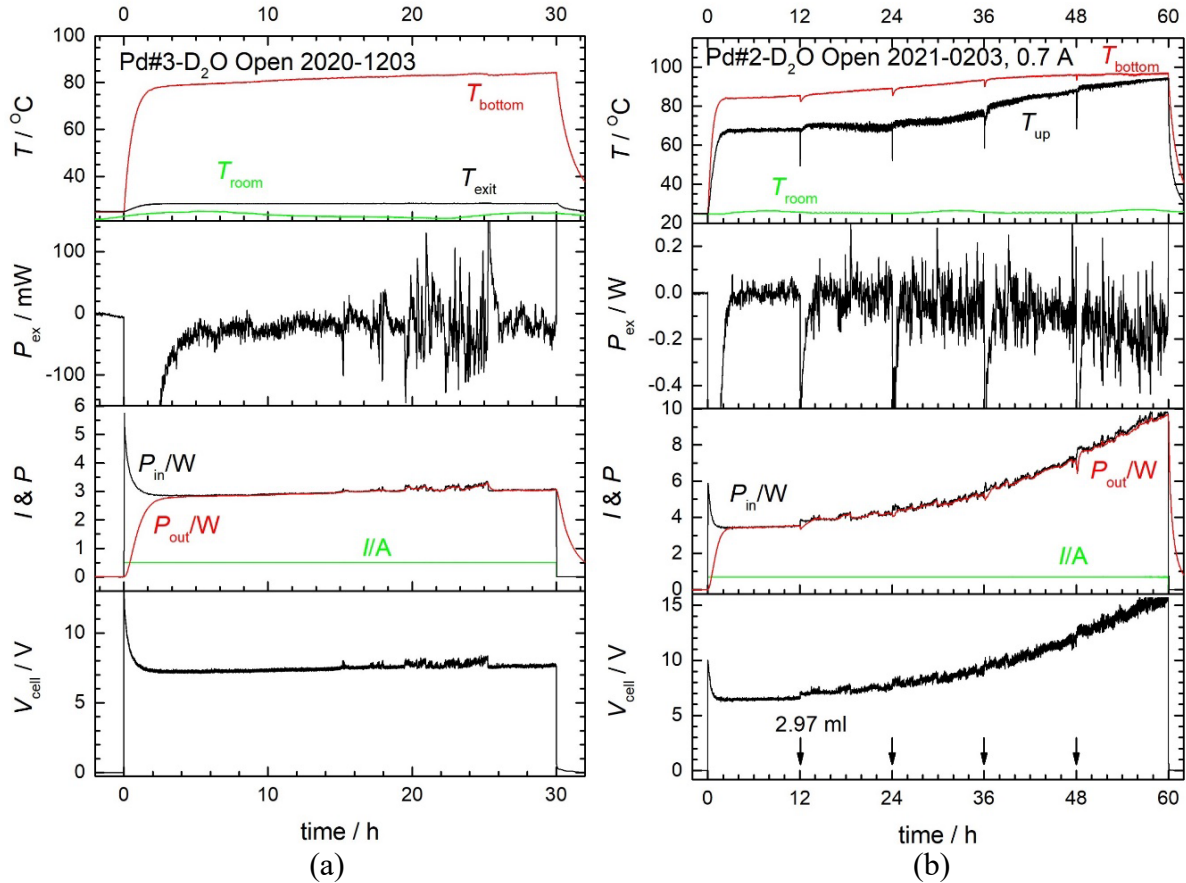


Figure 17. Occurrence of unsteady electrolysis in 19.5 to 25.3 h in Exp. #201203 (a) and changing from LTS (long term shift) to STF (short-term fluctuation) state after electrolysis of 12 h in Exp. #210203 (b).

We reanalyzed the data from 2018 to 2019 listed in Table 2 based on Eqs. (1) and (2) supposing that D₂O vapor was condensed in the closed Dewar or the sample chamber of the SEC. However, the resulting excess power is zero in the error range or negative values due to STF of electrolysis.

Rothwell had discussed the effects of insufficient data points on isoperibolic calorimetry recently^[17]. We extract the data of Exp. #210203 each minute to estimate energy balance. It is found that the output energy is the same as before. However, the input energy is 1,183.80 kJ, i.e., 0.76 kJ less than the original data listed in Table 7. It is verified that the data logging rate affects power balance in the unsteady electrolysis.

3.5. Problems of D₂O+LiOD solution

Besides the loss of D₂O by electrolysis and evaporation as discussed above, the loss of LiOD in the quartz tube is another factor affecting the steady state of electrolysis. We measured the conductivity of LiOD heavy water solution with a Mettler S230 conductivity meter to determine the concentration of LiOD before and after each run as reported in another paper of this volume^[18].

After each electrolysis experiment, we found a greyish sediment on the bottom of the cell, as shown in Fig. 18(a). Through precipitating, filtering and drying, this material was analyzed using PANalytical Empyrean powder XRD P2 and the result is shown in Fig. 18(b). The XRD pattern is the same as that of Li₂SiO₃^[19]. It was also found that white sediment occurred in the Pyrex tube after electrolysis in experiments from the years 2018 to 2019. This means that LiOD reacts with SiO₂ in the cell wall to form Li₂SiO₃, and this reaction is prominent especially when the temperatures are higher than 80°C as verified by others^[20].

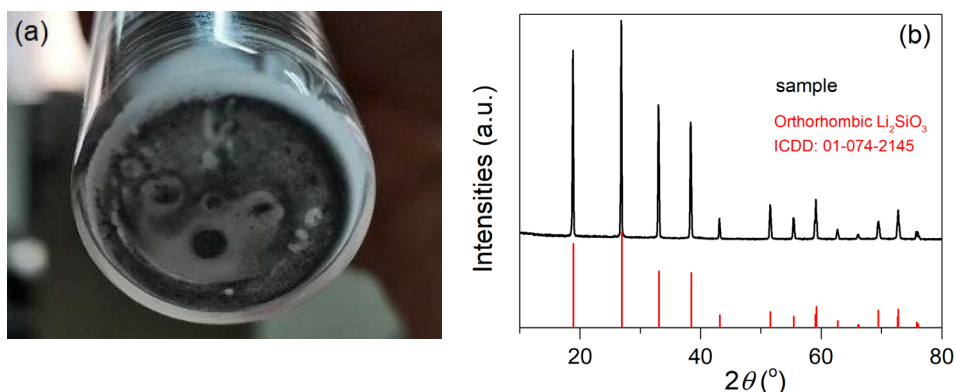


Figure 18. (a) The greyish sediment on the bottom of cell after electrolysis in Pd-D₂O system in Exp. #210107. This is the upward view of cell. (b) Comparison of XRD peaks of powders shown in (a) (black line) and standard Li₂SiO₃ (red line) ^[19].

4. Conclusion

In conclusion, 29 runs of Pt-D₂O(H₂O) open-electrolytic calorimetry and 24 runs of Pd-D₂O open-electrolytic calorimetry were conducted using an SEC from 2018 to 2021. There were signs of excess heat in Pd-D₂O systems. The Seebeck calorimetry of water open-electrolytic cell is not as simple as expected. In addition, a water reflux open-electrolytic cell was designed, and it has constant values of evaporation pressure and evaporation power, which is verified by mass loss measurement. What's more, excess heat was observed in both platinum-water and heavy water system with high reproducibility. Meanwhile, we obtained excess heat using two palladium alloy rods provided by Miles, however, the excess power and reproducibility are lower than that of platinum film.

Last but not least, this report is only about our primary results. Deeper studying and understanding on production of excess heat in palladium and platinum-water open-electrolytic systems have been and will be continued!

Acknowledgments

This work was supported by NSFC (21153003, 20973185) and 973 program of MOST in China (2009CB226113).

References

- [1] M. Fleischmann, S. Pons and M. Hawkins, Electrochemically induced nuclear fusion of deuterium. *J. Electroanal. Chem.* **261** (1989) 301–308. Erratum in **263** (1989) 187–188.
- [2] M. Fleischmann, S. Pons, M.W. Anderson, L.J. Li and M. Hawkins, Calorimetry of the palladium-deuterium-heavy water system. *J. Electroanal. Chem.* **287** (1990) 293–348.
- [3] M.C.H. McKubre, S. Crouch-Baker, R.C. Rocha-Filho, S.I. Smedley, F.L. Tanzella, T.O. Passell and J. Santucci, Isothermal flow calorimetric investigations of the D/Pd and H/Pd systems, *J. Electroanal. Chem.* **368** (1994) 55–66.
- [4] E. Storms, Use of a very sensitive Seebeck calorimeter to study the Pons–Fleischmann and Letts effects. *Proc. 10th Int. Conf. Cold Fusion*, P.L. Hagelstein and S.R. Chubb (Eds.), World Scientific, New York, 2006, pp. 183–197.
- [5] M.H. Miles, R.A. Hollins, B.F. Bush, J.J. Lagowski and R.E. Miles, Correlation of excess power and helium production during D₂O and H₂O electrolysis using palladium cathodes. *J. Electroanal. Chem.* **346** (1993) 99–117.
- [6] M.H. Miles, The Fleischmann–Pons calorimetric methods, equations and new applications. *J. Condensed Matter Nucl. Sci.* **24** (2017) 1–14.
- [7] M.H. Miles and M.A. Imam, Excess power measurements for palladium–boron cathodes. *J. Condensed Matter Nucl. Sci.* **29** (2019) 12–20.
- [8] M.H. Miles, The Thermoneutral potential in electrochemical calorimetry for the Pd/D₂O System. *J. Condensed Matter Nucl. Sci.* **33** (2020) 74–80.
- [9] W.-S. Zhang, J. Dash and Q. Wang, Seebeck envelope calorimetry with a Pd|D₂O+H₂SO₄ electrolytic cell. *Proc. 12th Int. Conf. Condensed Matter Nuclear Science*, Yokohama, Japan, Nov. 27 to Dec. 2, 2005, pp. 86–96.
- [10] W.-S. Zhang and J. Dash, Excess heat reproducibility and evidence of anomalous elements after electrolysis in Pd|D₂O + H₂SO₄ electrolytic cells. *Proc. 13th Int. Conf. Condensed Matter Nuclear Science*, Dagomys, Sochi, Russia, June 25 to July 1, 2007, pp. 202–216.
- [11] W.-S. Zhang, Characteristics of excess heat in Pd|D₂O+D₂SO₄ electrolytic cells measured by Seebeck envelope calorimetry. *Proc. 15th Int. Conf. Condensed Matter Nuclear Science*, Roma, Italy, Oct. 5-9, 2009, pp. 27–32.

- [12] J. Gao, W.-S. Zhang, J.-J. Zhang, Effects of D/Pd Ratio and cathode pretreatments on excess heat in closed Pd|D₂O + D₂SO₄ electrolytic cells. *J. Condensed Matter Nucl. Sci.* **24** (2017) 42–59.
- [13] M. Nakamura, K. Tamura S. Murakami, Isotope effects on thermodynamic properties: mixtures of $x(\text{D}_2\text{O or H}_2\text{O}) + (1 - x)\text{CH}_3\text{CN}$ at 298.15 K. *Thermochim. Acta* **253** (1995) 127–136.
- [14] W.-S. Zhang, A device and method for thermal power measurement. China Patent 201810191597.0.
- [15] J. Dash, Chemical changes and excess heat caused by electrolysis with H₂SO₄-D₂O electrolyte. *Proc. 6th Int. Conf. Cold Fusion*, Hokkaido, Japan, Oct. 13-18, 1996, pp. 477–481.
- [16] G. Lonchamp, J.-P. Biberian, L. Bonnetain, and J. Delepine, Excess heat measurement with Pons and Fleischmann type cells. *The 7th Int. Conf. on Cold Fusion, Vancouver, Canada: ENECO Inc., Salt Lake City, UT, 1998*, pp. 202–205.
- [17] J. Rothwell, Review of the calorimetry of Fleischmann and Pons. LENR-CANR.org, 2020.
- [18] H. Zhao, W.-S. Zhang, W.-Y. Xiao, Y. Chen, S. Qi, Conductivity and molar conductivity of LiOD heavy water solution. *Proc. 23th International Conference on Condensed Matter Nuclear Science*, Xiamen, China, June 7-9, 2021.
- [19] B.A. Maksimov, Yu.A. Kharitonov, V.V. Ilyukhin, N.V. Belov, The crystal structure of Li-metasilicate, Li₂SiO₃, *Dokl. Akad. Nauk SSSR* **178** (1968) 1309–1302.
- [20] B. Zhou, Z. Mao and M. Deng, Reaction of quartz glass in lithium-containing alkaline solutions with or without Ca, *R. Soc. Open Sci.* **5** (2018) 180797.